Research Article

Received: 30 June 2012 Revised: 14 November 2012 Accepted: 14 January 2013 Published online in Wiley Online Library:

(wileyonlinelibrary.com) DOI 10.1002/pi.4498

Fabrication of ferrogels using different magnetic nanoparticles and their performance on protein adsorption

Jimena S. Gonzalez,[a] Paula Nicolás,[b] María Luján Ferreira,[c] Marcelo Avena,[b] Verónica L. Lassalle[b]* and Vera A. Alvarez[a]

Abstract

Magnetic biomaterials were prepared using magnetite and chitosan-coated magnetite nanoparticles (CSNPs) dispersed in poly(vinyl alcohol) gels. Two different methods were developed to obtain ferrogels: *in situ* co-precipitation of magnetite (Ferro-IS) and by adding previously synthesized CSNPs to the neat matrix (Ferro-CSNPs). In both cases, the crosslinking was carried out by freezing – thawing (F-T). The as-prepared materials as well as precursor CSNPs were characterized by Fourier transform infrared spectroscopy, electronic microscopy (scanning and transmission), X-ray diffraction, ζ potential, dynamic light scattering, thermogravimetric analysis, differential scanning calorimetry and magnetic properties. The performance of these gels as protein adsorbents was evaluated. Batch adsorption experiments were carried out using bovine serum albumin (BSA) as a model. Substantially different adsorption behaviour was found using Ferro-IS and Ferro-CSNPs. This was assigned to dissimilar bonding mechanisms of BSA to the ferrogel matrix. Hence, biomaterials potentially useful in drug delivery as well as in protein purification fields may be prepared by a relatively simple, non-toxic and low cost method.

Supporting information may be found in the online version of this article.

Keywords: biomaterials; iron oxides; magnetic materials; adsorption; ferrogel; protein

INTRODUCTION

Ferrogels are stimuli-responsive polymers with promising uses in the biomedical area, i.e. as drug delivery devices.[1] They are a new kind of smart material that responds to an external non-uniform magnetic field, changing their volume or structure due to the coupling of magnetic and elastic properties (typical deformation patterns include elongation, rotation and torsion, coiling and bending of the polymer).[2,3] Ferrogels are commonly prepared using magnetic nanoparticles (NPs) and a polymer matrix.[4] One of the most widely used polymers for this purpose is poly(vinyl alcohol) (PVA), a highly biocompatible and hydrophilic, non-toxic and inexpensive polymer that can be easily processed.[5] PVA solutions may form hydrogels by a non-toxic method called freezing–thawing (F-T), which consists of consecutive cycles of freezing and thawing the polymer solutions.[6] All mentioned properties together have led to the use of PVA-based gels in a wide range of applications in the medical, pharmaceutical and packaging fields.[7]

Different kinds of magnetic devices based on hydrogels have been investigated. For instance, García-Cerdá *et al*.[8] prepared and characterized PVA – cobalt ferrite ferrogels by the casting method. Liu *et al*. synthesized chemically crosslinked ferrogels based on gelatine and magnetite NPs.[9] Satarkar and Hilt[10] produced temperature-responsive magnetic nanocomposites based on poly(*N*-isopropyl acrylamide) and magnetite. According to a literature survey, various methods have been developed to prepare ferrogels;[11] among them the synthesis of *in situ* ferrogels based on PVA is one of the most promising due to its simplicity. It has been well studied and reported in previous work.[12] Briefly, this paper deals with the synthesis of superparamagnetic ferrogels based on F-T of ferrofluids prepared from the *in situ* synthesis of iron oxide in the presence of PVA.[12]

Proteins play a key role in all biological organisms.[13] Bovine serum albumin (BSA) is of great importance in pharmacology as the conjugation of certain drugs to albumin decreases their toxicity.[14] The well-known structural and physical characteristics of BSA help in investigations of protein conformational changes with magnetite surfaces.[15] The ability of polymers to protect proteins from proteolysis and antibody neutralization *in vivo* in addition to supplying a controlled release vehicle is also known.[16,17] Hydrogels can occlude a large amount of water providing an aqueous

* *Correspondence to: Verónica. Lassalle, Institute of Chemistry of the South (Inquisur, Universidad Nacional del Sur – CONICET), Avda Alem 1253, Bahía Blanca (CP 8000), Argentina. E-mail: veronica.lassalle@uns.edu.ar*

a *Composite Materials Group (CoMP), Institute of Materials Science and Technology (INTEMA), University of Mar del Plata and National Research Council (CONICET), Solís 7575, B7608FLC, Mar del Plata, Argentina*

b *Institute of Chemistry of the South (Inquisur, Universidad Nacional del Sur – CONICET), Avda Alem 1253, Bahía Blanca, Argentina*

c *Pilot Plant of Chemical Engineering (PLAPIQUI), Universidad Nacional del Sur – CONICET), Camino La Carrindanga km 7, Bahía Blanca, Argentina*

environment that protects proteins.[18,19] Therefore, water-soluble proteins can easily diffuse through a hydrogel matrix with only its size as a restriction.[20] Generally, hydrogels adsorb proteins not only on their surface but also in their network[21] and the amount of protein adsorbed depends on the hydrogel water content (thus the crosslinked density).[22] The uptake of the protein appears to be directly dependent on the hydrogel structure and composition.[23] Much work has demonstrated that most of the water-soluble proteins will reside in water filled pores when incorporated into the matrix.[24,25]

The aim of this work was to formulate and characterize ferrogels for drug delivery and purification of proteins. Two different procedures were performed to obtain these materials, both based on the F-T method. Hence, two kinds of ferrogels were achieved, one containing raw iron oxide NPs and the other containing chitosan-coated NPs (CSNPs). These biomaterials were evaluated with regard to their ability to adsorb a model protein (BSA), aiming to determine the influence of the ferrogel structure on the adsorption capability. On the other hand, such assays were performed as a preliminary step to employing ferrogels with more complex medicaments as well as other proteins.

MATERIALS AND METHODS

Materials

PVA with average molecular weight-average molecular weight of 93 000 g mol^{-1} and a hydrolysis degree higher than 98%–99% was purchased from Sigma-Aldrich (Saint Louis, USA). CS, commercialized as Chitoclear, was provided by Primex (Siglufjordur, Iceland). BSA was supplied by Laboratorios Wiener (Buenos Aires, Argentina). Iron(II) sulfate, heptahydrated, and iron(III) chloride, hexahydrated, were purchased from Cicarelli Laboratory (Buenos Aires, Argentina), hydrochloric acid was from Biopack (Argentina) and ammonium hydroxide was provided by Anedra Laboratory (Buenos Aires, Argentina).

Synthesis of magnetic nanoparticles

Bare magnetite nanoparticles

Magnetite was synthesized by a co-precipitation method.[26] In brief, 3.254 g of $FeCl_3.6H_2O$ (12.1×10^{-3} mol Fe^{3+}) and 1.789 g of $FeSO_4.7H_2O$ (6.46×10^{-3} mol Fe^{2+}) were dissolved in 100 mL of distilled water. The solution was stirred at 70 °C under a N_2 atmosphere for 25 min. Then, 25 mL of NaOH (5 mol L^{-1}) was added to precipitate the oxide. The addition of the alkali was performed at a rate of 1 mL min^{-1} in order to minimize the magnetite (Fe_3O_4) aggregation. The solution changed from brown, in the initial addition stages, to black at the end of the NaOH addition. The mixture was allowed to complete magnetite formation for 30 min. The dark dispersion obtained was filtered, and three washing steps were performed using bidistilled water. The resultant solid was dried in an oven at 45 °C overnight producing 1 g of magnetite.

Chitosan-coated magnetite nanoparticles

Magnetite nanoparticles (75 mg) were dispersed in 10 mL of NaCl 0.1 mol L^{-1} solution[27,28] acidulated with acetic acid (10 vol%) (pH 4) and containing 25 mg of CS. The NaCl was used to reduce the electrostatic repulsion between the NPs.[29] The dispersion was performed under magnetic stirring at room temperature. NaOH 0.1 mol L^{-1} (5 mL) was added at a controlled rate (around 0.5 mL min^{-1}) in order to precipitate the CS. The mixture was magnetically stirred for 30 min and sonicated for 60 min. Solid CSNPs were isolated after two decantation and centrifugation cycles.

Preparation of ferrogels

Two kinds of ferrogels were prepared in the present work, the first, Ferro-IS, using an *in situ* method and the other, Ferro-CSNPs, by addition of previously prepared CSNPs (as described above) in the PVA matrix. The nominal weight of iron oxide NPs was kept constant (6 wt%) with respect to the PVA weight, in both cases.

For comparison, samples of hydrogels without NPs were prepared following the same methodology, without the addition of iron salts or CSNPs.

Preparation of Ferro-IS

PVA aqueous solution (100 mL of 10 wt%) was added to a solution containing a stoichoimetric ratio (2:1) of $FeCl_3.6H_2O$ (1.44 g) and $FeSO_4.7H_2O$ (0.72 g) in acidic medium (to avoid oxidation of Fe(II)) at 85 °C with slow magnetic stirring (250–300 rpm) for 4 h. After cooling to room temperature, NH_3 was added until pH 10 was reached, inducing basic co-precipitation of magnetic NPs. The amount of Fe^{2+}/Fe^{3+} solution was enough to obtain 6 wt% NPs relative to the PVA nominal weight.

To obtain ferrogels, crosslinking was carried out on flat anti-adherent moulds using 10 mL of the previous solution. The moulds with the samples were frozen in a commercial freezer for 1 h at −18 °C and then thawed at 25 °C (room temperature) for the same time in order to induce crosslinking. This F-T cycle was repeated three times. The film obtained was dried in an oven at 37 °C until constant weight. This ferrogel was exhaustively characterized in our previous work.[12]

Preparation of Ferro-CSNPs

A 10 wt% PVA aqueous solution was obtained by dissolving 0.5 g PVA in 4.5 mL of distilled water at 85 °C for 3 h under low magnetic stirring (250–300 rpm). Then, a proper amount (46.15 mg) of CSNPs (dispersed in water) was added in order to obtain ferrogels with 6 wt% iron oxides, relative to the initial amount of PVA. This mixture was stirred at 300 rpm for 1 h at 85 °C. The crosslinking procedure was similar to that described above. These materials were dried in an oven at 37 °C until constant weight.

Characterization

Fourier transform infrared (FTIR) spectroscopy

An FTIR (DRIFTS) Thermo Scientific Nicolet 6700 spectrometer was used for recording 100 scans in the range 4000–400 cm^{-1} with a resolution of 4 cm^{-1}. This technique was employed to corroborate the presence of polymeric moieties in the magnetite as well as to confirm the adsorption of proteins on the magnetic supports.

Electron microscopies (SEM and TEM)

A scanning electron microscope (JEOL35-CF1983-Japan) and transmission electron microscope (JEOL100-CX II-Japan, CRIBABB–CCT, Bahía Blanca, Argentina) were employed to examine the morphologies. In the case of SEM analysis, ferrogel samples were swelled in distilled water, cryo-fractured in liquid nitrogen and lyophilized before testing. For TEM, ferrogel samples were cryo-fractured in a cryo-ultramicrotome before testing.

UV–visible spectrophotometry

A UV–visible spectrophotometer Shimadzu 160 (Japan), equipped with a computer system for data acquisition, was used to quantify the adsorbed protein.

ζ potential and particle size measurements

A Malvern Zetasizer was employed to measure the ζ potential and the hydrodynamic particle diameter. Dispersions of the magnetite NPs, CSNPs and pure polymers were prepared in a mixture of ethanol and bidistilled water 50/50 (pH approximately 7.6–8) to measure ζ. The same dispersion as well as others prepared in organic medium (acetone) were employed to measure particle sizes.

Thermogravimetric analyses

TGA studies were carried out in a Shimadzu TGA-DTGA 50. All dried samples (37 °C, until constant weight) were scanned from room temperature to 900 °C at 10 °C min^{-1} in air. The iron oxide content and the degradation temperature (T_p) were obtained from the acquired curves. The iron oxide content is the result of the total oxidation of the sample, determined as the residual weight at 900 °C.

Differential scanning calorimetry

DSC measurements were carried out in a Shimadzu DSC-50. Samples were heated from room temperature to 250 °C at a rate of 10 °C min^{-1} in a nitrogen atmosphere. The melting temperature (T_m) was taken from the DSC curve. The degree of crystallinity (X_{cr}) was calculated from the equation

$$X_{cr}\ \% = \frac{\Delta H}{w_m \Delta H_c} \times 100 \quad (1)$$

where ΔH was determined by integrating the area under the melting peak over the range 190–240 °C, ΔH_c is the heat required for melting a 100% crystalline PVA sample (138.6 J g^{-1})[30] and w_m is the weight fraction of PVA (obtained from TGA).

Magnetic properties

The magnetic behaviour of the materials was qualitatively examined in terms of their response to a permanent magnetic field generated by Nd magnets.

Adsorption experiments

Batch adsorption experiments were performed in 10 mL vials by adding 100 mg of each ferrogel cut in small pieces to 5 mL of bidistilled water containing the corresponding amount of BSA. These vials were stirred in a thermostatic bath for 180 min at 37 °C (physiological temperature). The BSA adsorbed on the solid supports was measured from the decrease of protein concentration in the supernatant using UV–visible spectrophotometry.[31] This concentration was measured at 276 nm, which is the typical absorption wavelength of this protein.[32] A calibration curve of BSA is included in the Supporting Information. The loading efficiency (LE%), which is the percentage of adsorbed protein relative to the initial amount of BSA, was calculated using

$$LE\ \% = \frac{c_{BSA,i} - c_{BSA,f}}{c_{BSA,i}} \times 100 \quad (2)$$

where $c_{BSA,i}$ is the initial BSA concentration (before adsorption) and $c_{BSA,f}$ is the final BSA concentration (after the incubation period).

The pH of the solution was the physiological pH (*ca* 7.4), although additional studies were carried out near the isoelectric point of BSA (*ca* 4.8).

Adsorption kinetics were studied following the previously described procedure, using a fixed amount of BSA (30 mg) and withdrawing 200 μL aliquots of adsorption supernatant at different intervals of time. Each adsorption experiment was carried out in triplicate and an average was calculated.

RESULTS AND DISCUSSION

Characterization of magnetic devices

Magnetic nanoparticles

The modification of NPs obtained by co-precipitation was effectively achieved using CS as a coating. Figure 1 shows FTIR-DRIFTS spectra of NPs of bare magnetite, CS and the CSNPs. The signals assigned to the functional groups of biopolymer are present in the CSNP spectrum, at around 1100, 1640 and 3400 cm^{-1}, while the typical band of Fe–O is also observed at 570 cm^{-1}.[33] These spectra reveal that both magnetic and polymeric components coexist in the CSNPs.

Dynamic light scattering (DLS) reveals that bare magnetite NPs and CSNPs have significant differences in their hydrodynamic diameter as displayed in Table 1. This could be a consequence of CS incorporation on the magnetite particles. Iron oxide particles only form a relatively stable dispersion in aqueous media at pH ≈ 7.4. In contrast, dispersing magnetite NPs in an organic medium (acetone) led to aggregates of various sizes increasing the polydispersity, which inhibits the possibility of obtaining a reliable value for hydrodynamic size.

It is clear from the data in Table 1 that the capability of NPs to disperse in hydrophilic/hydrophobic media is also altered by the polymer incorporation. It is worth noting that the evaluation of hydrodynamic sizes in different media was strongly associated with the future biomedical applications of these materials.

Particles containing CS are highly aggregated in water dispersion, leading to hydrodynamic diameters higher than 1 μm. In contrast, the same particles dispersed well in organic medium exhibiting lower aggregation levels. This is because of the nature of the CS-Fe interaction (from magnetite [MAG]), where it is evident that uncharged functional groups from CS remain

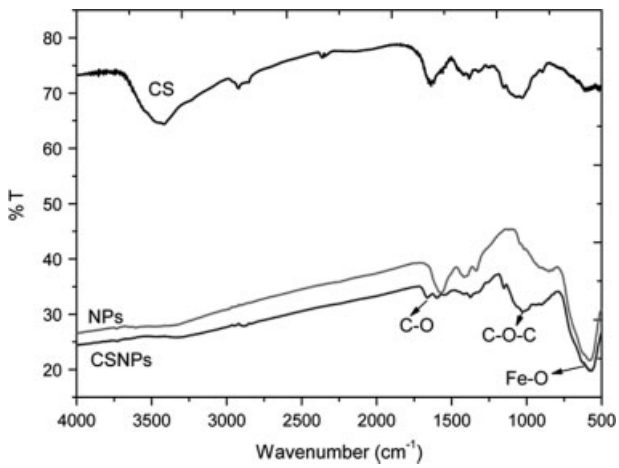

Figure 1. FTIR-DRIFTS spectra of magnetite NPs, pure CS and CSNPs.

Table 1. Hydrodynamic diameter, polydispersity index (PDI) and ζ of raw magnetite and CSNPs as a function of the dispersant medium

NPs	Dispersant	Hydrodynamic diameter (nm)	PDI	ζ (mV)[a]
Magnetite	Water	417	0.25	−8.48
	Acetone	[b]	0.50	
CSNPs	Water	1297	0.40	−2.49
	Acetone	441	0.40	

[a] Dispersions prepared in bidistilled water (pH 7.5).
[b] It does not meet the quality criteria. The sample was very polydisperse with large amounts of aggregates.

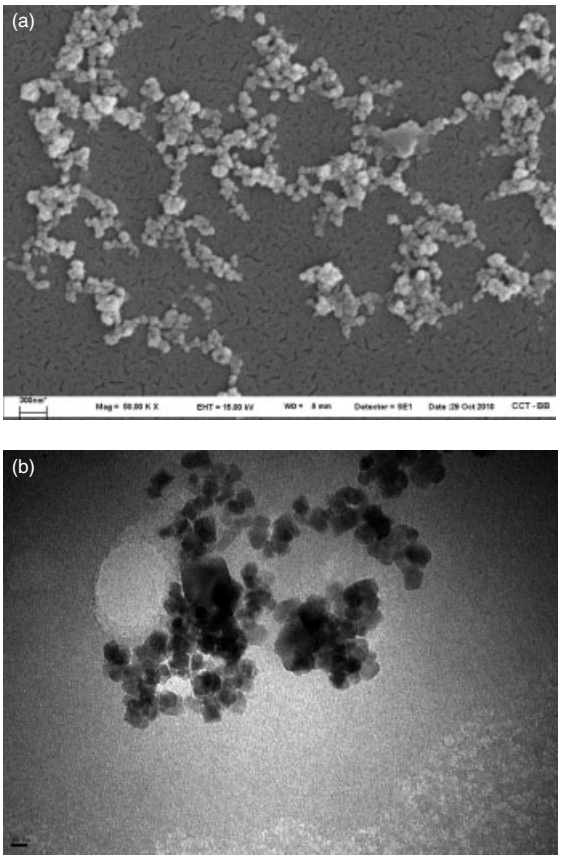

Figure 2. (a) SEM and (b) TEM images of CSNPs.

exposed to the surface hindering their dispersion in a hydrophilic medium (water). Hydrophobic moieties from the biopolymer remain exposed, maintaining their affinity with non-polar solvents.

With regard to the surface charge, untreated magnetite NPs present a negative surface charge in distilled water at pH $\approx$ 7.4 (the conditions fixed for ζ measurement). The surface Fe atoms from magnetite act as Lewis acids and therefore coordinate with molecules that donate one pair of electrons (Lewis bases).[34] Moreover, in aqueous solutions, Fe atoms coordinate with hydroxyl groups (OH) from water leading to surface hydroxyl functionalized iron oxide. In the conditions of ζ measurements, the magnetite surface is negatively charged due to the OH deprotonation.[35] The incorporation of CS partially neutralizes this surface charge leading to a slight increase in ζ.

Table 2. Thermal properties of gels

Sample	Fe (%)	T_p (°C)	X_{cr} (%)	T_m (°C)
Hydrogel	0	282.5	31.8	220.0
Ferro-IS	8.6	318.1	26.2	215.0
Ferro-CSNPs	10.7	336.6	56.5	229.5

Fe, iron oxide content; T_p, degradation temperature; X_{cr}, degree of crystallinity; T_m, melting temperature.

The micrographs of CSNPs obtained by SEM and TEM reveal that the particles are aggregated. Individual particles could be distinguished, with a diameter in the range 50–100 nm (Fig. 2). Moreover, TEM shows the magnetic core of CSNPs, which is smaller than 10–20 nm. The particle size obtained by DLS is usually higher than that corresponding to TEM. This could be attributed to the agglomeration caused by magnetostatic interaction of the magnetic particles.[36]

The magnetostatic interactions between particles is of the magnetic dipole–dipole type, which causes their attraction to each other and their agglomeration, even forming closed rings and long open loops. As the diffusion coefficient of agglomerated particles is lower than that of single particles, the diameter measured by DLS is higher than that by TEM. No loop and ring structures are observed in TEM; they are probably destroyed by evaporation of the dispersant and the drying forces during sample preparation.[37]

Ferrogels

Both kinds of ferrogel film discs, with a diameter of 8 cm and a thickness of 300 µm (mould size, measured with a caliper),

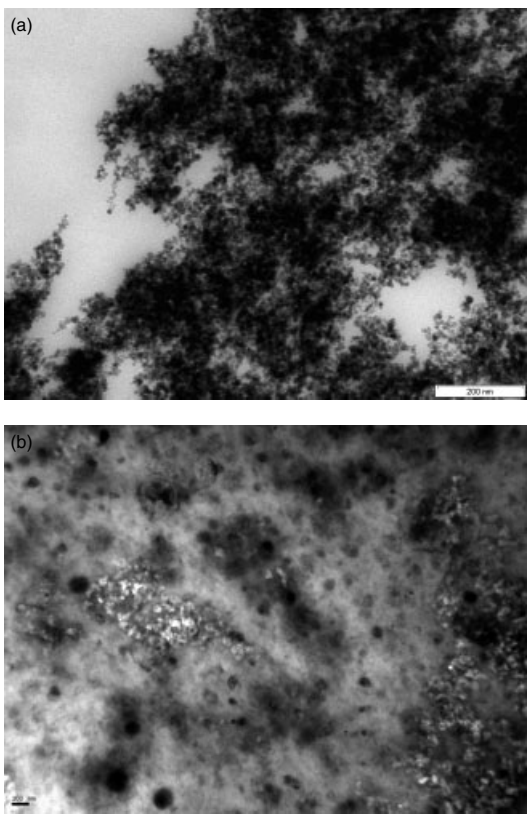

Figure 3. TEM images of (a) Ferro-IS and (b) Ferro-CSNPs.

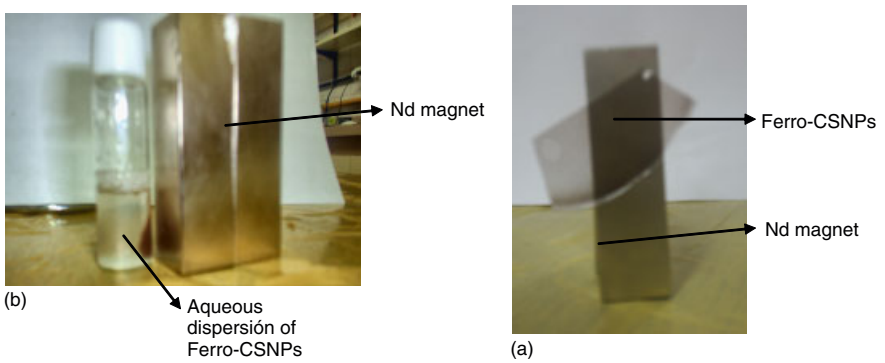

Figure 4. (a) Photograph of Ferro-CSNPs exposed to a high potency magnet; (b) dispersion of Ferro-CSNPs in bidistilled water (at physiological pH) exposed to a high potency permanent magnet.

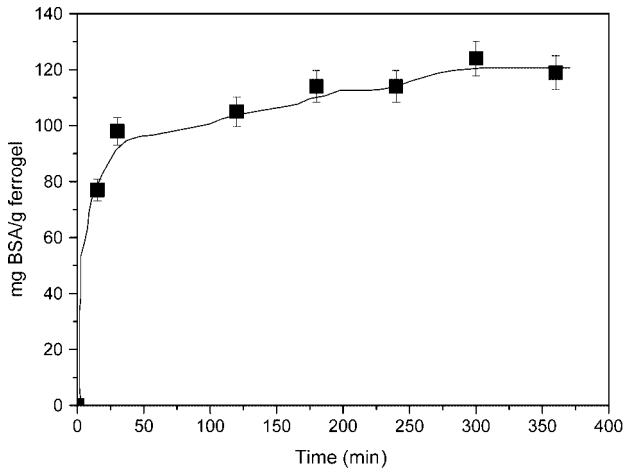

Figure 5. Adsorption kinetics of BSA on Ferro-IS.

were dried in an oven at 37 °C to constant weight and then examined. Ferro-IS was exhaustively characterized in our previous work.[12]

The thermal characteristics of the prepared hydrogels and ferrogels are given in Table 2. These data show that Ferro-CSNPs have better crystallization properties, higher crystallinity degree and higher melting temperature than Ferro-IS and hydrogels (the DSC and TGA curves are displayed in the Supporting Information). These results may be assigned to the interaction of CSNPs with PVA by hydrogen bonding through the carboxyl and /or amino groups of the CS and OH groups of PVA.[38] This interaction of CSNPs with the PVA chains is strong and facilitates nucleation of large crystals in the PVA matrix, explaining the high values of X_{cr} and T_m for these nanocomposites.[39,40] The shift of Ferro-CSNPs to higher melting temperature than Ferro-IS further indicates the strength of the interactions between the ferrogel components (CS and PVA).[41] In addition, the weight of iron oxide retained was higher in Ferro-CSNPs, also due to the better interaction between the PVA chains and the CS on the magnetite surface.

The TEM micrograph of Ferro-IS (Fig. 3(a)) shows a good dispersion of magnetite NPs on the PVA matrix, with typical sizes around 10 nm. The stabilization properties of PVA avoid initial aggregation of crystals during co-precipitation.[12] In the case of Ferro-CSNPs, the TEM micrograph (Fig. 3(b)) shows a substantially different morphology. A more heterogeneous distribution of CSNPs is observed as well as the presence of porous regions. The observed morphology could be ascribed to the different sizes of CSNPs and the possibility of interactions of a different nature.

The magnetic properties of ferrogels were macroscopically evaluated. The response of the formulated materials against a permanent magnet is demonstrated in Fig. 4, which shows the magnetic character of these materials in a qualitative way. The magnetic behaviour of CSNPs and Ferro-IS was exhaustively analysed in previous work.[12,42] The Ferro-IS and CSNPs present almost complete superparamagnetic behaviour at room temperature, with very low values of coercivity (10 Oe for Ferro-IS and less than 5 Oe for CSNPs) and saturation magnetization of roughly 60 emu g^{-1} for Ferro-IS and 40 emu g^{-1} for CSNPs.The Ferro-CSNP SQUID assays are currently being continued .

Adsorption of BSA

Effect of the incubation time: adsorption kinetics

The adsorption kinetics of BSA were investigated at physiological pH (7.4 – 7.8) with a feed concentration of 6000 mg BSA L^{-1} solution. The recorded data resulting from the immersion of Ferro-IS samples in this solution are given in Fig. 5, which shows that the concentration of BSA adsorbed per gram of ferrogel in incubation remains almost constant after 180 min. Higher adsorption times do not increase the amount of BSA linked to the ferrogels. This experimental evidence led us to conclude that 180 min is the equilibrium time during which BSA adsorption on ferrogels takes place; consequently it was adopted in the following experimental assays. These results agree with our previous work[43] as well as with other published work using different supports. For instance, Xu *et al*. found that this time ensured the maximum amount of protein adsorbed on porous polyethylene membranes.[44]

Effect of pH

Modification of the pH of the adsorption medium did not induce significant changes in the maximum amount of BSA incorporated

Table 3. Percentage of adsorbed BSA after 180 min as a function of pH

pH	Ferrogel weight (mg)	Initial weight of BSA (mg)	BSA/ferrogel ratio (mg g^{-1})	BSA absorbed (%)
4.0	102	30	146 ± 3	50
7.8	101	30	151 ± 5	51

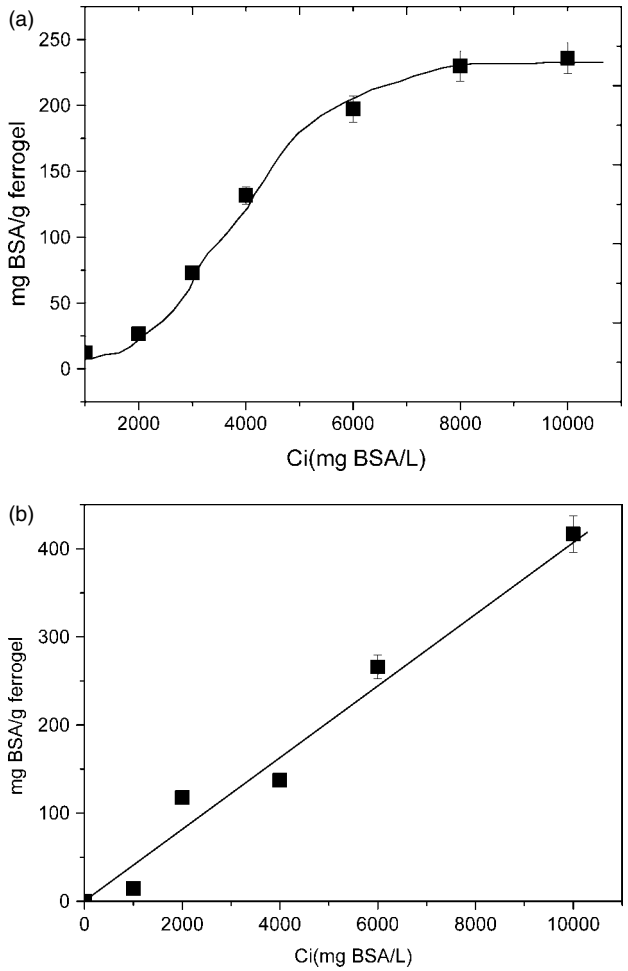

Figure 6. Adsorption profiles of BSA: (a) Ferro-IS; (b) Ferro-CSNPs.

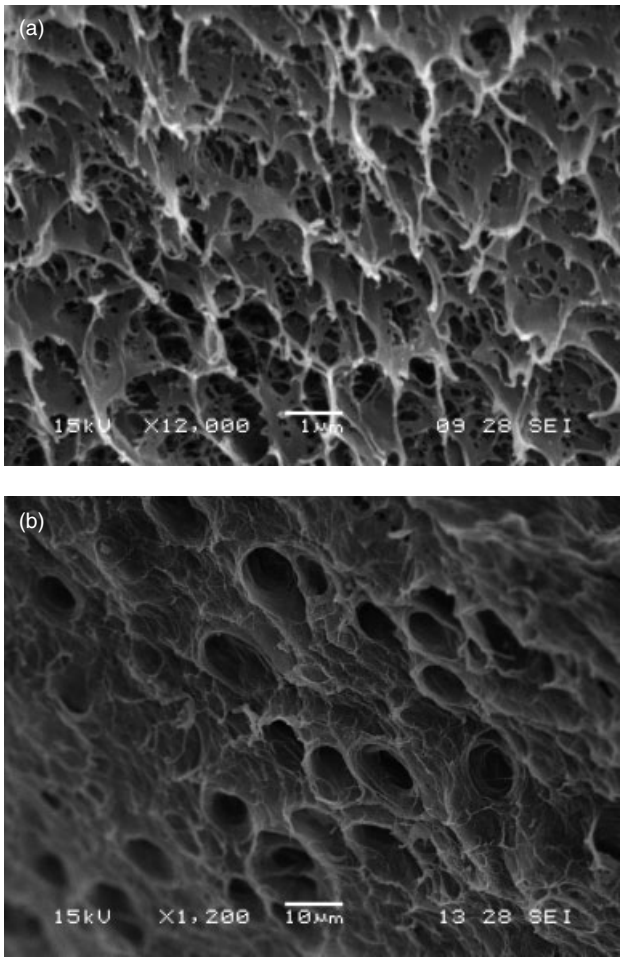

Figure 7. SEM images of (a) Ferro-IS and (b) Ferro-CSNPs.

on Ferro-IS, as demonstrated by the results included in Table 3. Such data are expressed in terms of loading efficiency.

BSA is an amphoteric protein due to the presence of an NH_2 and a COOH group in its molecular structure. It shows a different net charge at different pH values. Its isoelectric point (p*I*) is 4.8, suggesting that BSA has a positive charge below p*I* and negative above it. The measured ζ of BSA at pH 7.8 was -18 mV (data not shown) and is in accordance with available literature.[45]

From the data included in this section, the main interactions between ferrogel and protein are not of an electrostatic nature, which is in agreement with published papers. For instance, Sivudu and Rhee[46] studied BSA adsorption on acrylamide based gels at different pH. They found maximum BSA adsorption levels at neutral pH. A possible explanation is that the polymer network swells more and the iron oxide is more available, which enhances adsorption capability at pH 7.[46] Furthermore, the possibility of BSA interacting with available OH groups from PVA through hydrogen bonding or van der Waals forces has been previously reported, and that the pH of the medium defines the shape adopted by the protein during adsorption. Thus BSA adsorption depends, not only on the electrostatic and hydrophobic interactions, but also on the conformational alteration of the protein molecules.[47]

Effect of the nature of the ferrogel

Results from the adsorption of BSA on Ferro-IS and Ferro-CSNPs are displayed in Figs 6(a) and 6(b) respectively in terms of adsorption profiles. It is important to highlight that in this work the main aim was to compare the performance of the prepared materials for BSA adsorption. Therefore the adsorption profiles were evaluated in place of adsorption isotherms. However, to show the difference, the adsorption isotherm of Ferro-IS is included in the Supporting Information.

The adsorption profiles using the two supports were found to be markedly dissimilar. In the case of Ferro-IS, its profile yields a plateau at about 228 mg of adsorbed BSA per gram of ferrogel that corresponds to the maximum amount of protein adsorbed and the saturation of the available sites for BSA incorporation, under the experimental conditions selected in this work. Employing Ferro-CSNPs the adsorption profile shows an almost linear growth of the adsorbed BSA as a function of the initial amount of protein, in the concentration range used. This means that the adsorption capacity increases with increasing initial BSA concentration, reaching a maximum of 400 mg of adsorbed BSA per gram of ferrogel. Moreover, saturation of available ferrogel sites does not occur under our experimental conditions. A similar behaviour has been observed during adsorption of BSA onto magnetic CS NPs.[48] Wang *et al*. obtained a good linear relationship between the initial concentration of protein and the amount adsorbed, expressed as milligrams BSA per gram of support. Therefore the authors proposed that the Freundlich model was the most suitable to describe BSA adsorption onto magnetic CS particles.[48]

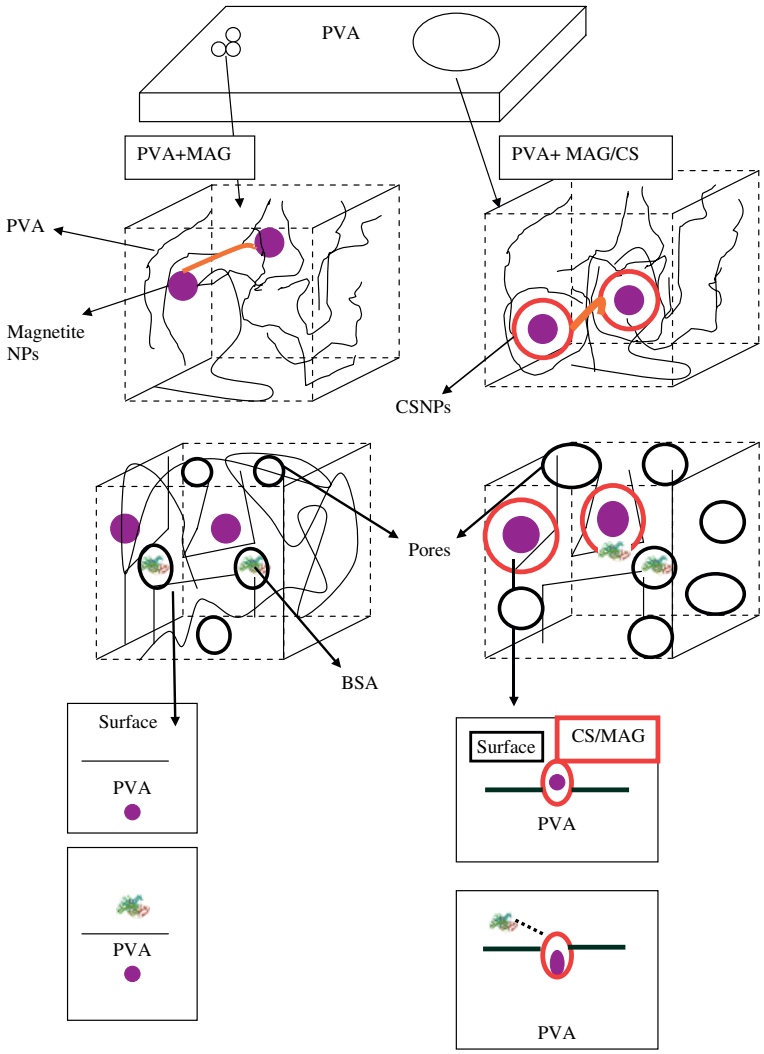

Figure 8. Schematic representation of BSA interactions in different ferrogel environments.

Comparing the performance of the two supports in their ability to bind the protein, it is observed that the adsorption capability was enhanced by75% when Ferro-CSNP was used. This behaviour can be explained in terms of the different kinds of protein – support interactions and the available adsorption sites in each case.[49] Analysis by SEM demonstrated that completely different morphologies are achieved using the two procedures to obtain ferrogels. Figure 7 includes micrographs of (a) Ferro-IS and (b) Ferro-CSNPs. From these figures it can be seen that although both formulations are porous they differ drastically in their pore size and distribution. The pore diameters for Ferro-CSNPs and Ferro-IS were measured by Image Pro Plus software and the results were $7.8 \pm 1.6\,\mu m$ and $0.4 \pm 0.15\,\mu m$ respectively. In the case of Ferro-CSNPs the pore size is almost an order of magnitude larger than for Ferro-IS. According to the available literature, protein could be linked to ferrogels by occupying the gel's pores and interacting with PVA chains.[50] Thus it is clear that the structure of PVA ferrogel plays a key role in the efficiency of protein adsorption, in agreement with other authors.[24,25] These studies involved fluorescent probes and the use of a confocal scanning laser microscope during the incorporation of BSA on PVA networks. They reported that most of the protein resides in the water filled pores when incorporated into the matrix. Therefore, the dissimilar behaviour of Ferro-IS and Ferro-CSNPs could be attributed to the difference in the PVA filled space.

Based on the available literature, another potential factor influencing BSA adsorption is related to new interactions between CS surface exposed moieties from CSNPs, in Ferro-CSNPs, and protein.

The presence of biopolymer offers greater possibilities for hydrogen bonding interactions due to the large amount of NH_2 and OH groups in its networks. Hence functional groups on CS could provide extra linkage sites for protein binding among pores available in the gel structure. The excellent capability of CS coated magnetic NPs to adsorb BSA has been reported in the literature.[43,48] The proposed ferrogel structures as well as proposed BSA interactions with both ferrogels are illustrated in Fig. 8.

CONCLUDING REMARKS

Two simple and low cost methods were employed to prepare PVA based ferrogels. The method of incorporation and the nature of the magnetic components play a key role in the final structure and properties of the ferrogels. Such materials are demonstrated to be highly suitable for adsorption of a model protein through a simple

physical adsorption method. It was verified that the adsorption capability is independent of the pH of the medium.

In addition, it was demonstrated that the mechanism of adsorption is basically governed by the porous structure of the ferrogel, which is substantially different in the two cases. Therefore notably dissimilar BSA adsorption profiles were reached using Ferro-IS and Ferro-CSNPs.

These preliminary results are very promising with regard to the possibility of employing these systems not only as drug delivery devices but also as biosensors, or even in the purification of proteins.

ACKNOWLEDGEMENTS

The authors gratefully acknowledge the financial support of CONICET, UNMdP and UNS.

SUPPORTING INFORMATION

Supporting information may be found in the online version of this article.

REFERENCES

1 Zhao X, Kim J, Cezar CA, Huebsch N, Lee K, Bouhadir K, *et al*, *Proc Natl Acad Sci U S A* **108**: 67–72 (2011).
2 Szabo D, Czako-Nagy I, Zrınyi M and Vertes A, *J Colloid Interf Sci* **221**: 166–172 (2000).
3 Zubarev AY, *Soft Matter* **8**: 31–74 (2012).
4 Qin J, Asempah I, Laurent S, Fornara A, Muller RN and Muhammed M, *Adv Mater* **21**: 1354–1357 (2009).
5 Krumova M, López D, Benavente R, Mijangos C and Peresa JM, *Polymer* **41**: 9265–9272 (2000).
6 Gonzalez JS and Alvarez VA, Poly(vinylalcohol) hydrogels: Influence of Processing Variables on General Behavior and Drug Release Device Performance in *Advances in Materials Science Research*, ed. by Maryann C. Wythers. Nova Science Publishers, New York, Vol. **10**, pp. 265–285 (2011).
7 Lee MK, Bae H, Lee S, Chung NO, Lee H, Choi S, *et al*, *Macromol Res* **19**: 130–136 (2011).
8 García-Cerdá LA, Escareño-Castro MU and Salazar-Zertuche M, *J Non-Cryst Solids* **353**: 808–810 (2007).
9 Liu TY, Hu SH, Liu KH, Liu DM and Chen SY, *J Magn Magn Mater* **304**: e397–e399 (2006).
10 Satarkar NS and Hilt JZ, *J Control Release* **130**: 246–251 (2008).
11 Gonzalez JS, Hoppe CE and Alvarez VA, Poly (vinyl alcohol) Ferrogels: Synthesis and Applications in *Advances in Materials Science Research*, ed. by Maryann C. Wythers. Nova Science Publishers, New York, Vol. **13**, Ch. 8 (2012).
12 Gonzalez JS, Hoppe CE, Muraca D, Sánchez FH and Alvarez VA, *Colloid Polym Sci* **289**: 1839–1846 (2011).
13 Kobsa S and Saltzman WM, *Pediatr Res* **63**: 513–519 (2008).
14 Hansen KU, *Pharmacol Rev* **33**: 17 (1981).
15 Borah BM, Saha B, Kumar Dey S and Das G, *J Colloid Interf Sci* **349**: 114–121 (2010).
16 Lee KY and Yuk SH, *Prog Polym Sci* **32**: 669–697 (2007).
17 Hassan CM, Stewart JE and Peppas NA, *Eur J Pharm Biopham* **49**: 161–165 (2000).
18 Prokop A, Kozlov E, Carlesso G and Davidson J, *Filled Elastomers Drug Delivery Systems in Advances in Polymer Science*, ed. by Arora M. Springer, Berlin, pp. 119–173 (2002).
19 Lee F, Chung JE and Kurisawa M, *J Control Release* **134**: 186–193 (2009).
20 Lee KY and Mooney DJ, *Chem Rev* **101**: 1869–1879 (2001).
21 Kulik E and Ikada Y, *J Biomed Mater Res* **30**: 295–304 (1996).
22 Goda T, Matsuno R, Konno T, Takai M and Ishihara K, *J Biomed Mater Res B* **89**: 184–190 (2009).
23 Holly FJ, *J Polym Sci Pol Sym* **66**: 409–417 (1979).
24 Li JK, Wang N and Wu XS, *J Control Release* **56**: 117–126 (1998).
25 Ficek BJ and Peppas NA, *J Control Release* **27**: 259–264 (1993).
26 Gaihre B, Khil M, Lee D and Kim H, *Int J Pharm* **365**: 180– 188 (2009).
27 Signini R and Campana Filho SP, *Polym Bull* **42**: 159–166 (1999).
28 Schatz C, Pichot C, Delair T, Viton C and Domard A, *Langmuir* **19**: 9896–9903 (2003).
29 Klinkesorn U and Namatsila Y, *Food Hydrocoll* **23**: 1374–1380 (2009).
30 Mallapragada SK and Peppas NA, *J Polym Sci B* **34**: 1339–1346 (1996).
31 Lassalle VL and Ferreira ML, *J Chem Technol Biot* **85**: 1588–1596 (2010).
32 Lassalle VL, Pirillo S, Rueda E and Ferreira ML, *Curr Top Anal Chem* **8**: 83–93 (2011).
33 Nyquist R and Kagel R, *Infrared Spectra of Inorganic Compounds*, Academic Press, New York (1971).
34 Tombacz E, Majzik A, Horvat ZS and Illés E, *Rom Rep Phys* **58**: 281–286 (2006).
35 Cornell RM and Schertmann U, Iron Oxides in the Laboratory: Preparation and Characterization, VCH Publishers, Weinheim (1991).
36 Maity D and Agrawal C, *J Magn Magn Mater* **308**: 46–55 (2007).
37 Chantrell A, Popplewell J and Charles W, *J Appl Phys* **53**: 2742–2744 (1982).
38 Zheng H, Du Y, Yu J, Huang R and Zhang L, *J Appl Polym Sci* **80**: 2558–2565 (2001).
39 Mc Gann MJ, Higginbotham CL, Geever LM and Nugent MJD, *Int J Pharm* **372**: 154–161 (2009).
40 Udrea LE, Hritcu D, Popa MI and Rotariu O, *J Magn Magn Mater* **323**: 7–13 (2011).
41 Lewandowska K, *Thermochim Acta* **493**: 42–48 (2009).
42 Nicolas P, Saleta M, Troiani H, Zysler R, Lassalle V and Ferreira ML, *Acta Biomater* **9**: 4754–4762 (2013).
43 Lassalle V, Zysler R and Ferreira ML, *Mater Chem Phys* **130**: 624–634 (2011).
44 Xu T, Fu R and Yan AL, *J Colloid Interf Sci* **262**: 342–350 (2003).
45 Peters T Jr, *Adv Protein Chem* **37**: 161–245 (1985).
46 Sivudu KS and Rhee KY, *Colloids Surfaces A* **349**: 29–34 (2009).
47 Fair BD and Jamieson AM, *J Colloid Interf Sci* **77**: 525–534 (1980).
48 Wang Y, Wang X, Luo G and Dai Y, *Bioresource Technol* **99**: 3881–3884 (2008).
49 Dergunov SA and Mun GA, *Radiat Phys Chem* **78**: 65–68 (2009).
50 Liu R, Shen X, Jiang C, Songa F and Li H, *J Alloys Compd* **511**: 163–168 (2012).

Published online in Wiley Online Library:

(wileyonlinelibrary.com) DOI 10.1002/pi.4498

Research Article

Ferrogels of polyvinilalcohol and magnetic nanoparticles (NPs) were synthesized using different kinds of magnetic particles. Biomaterixsals obtained were found suitable for adsorption of a model protein.

Fabrication of ferrogels using different magnetic nanoparticles and their performance on protein adsorption 000

Jimena S. Gonzalez, Paula Nicolás, María Luján Ferreira, Marcelo Avena, Verónica L. Lassalle* and Vera A. Alvarez